J. Water Environ. Nanotechnol., 4(4): 285-295 Autumn 2019

ORIGINAL RESEARCH PAPER

Nitrogen doped porous carbon derived from polyaniline for CO_2 adsorption

Soodabeh Khalili, Mohsen Jahanshahi*

Department of Chemical Engineering, Babol Noshirvani University of Technology, Shariati Av., Babol, Iran

Received: 2019-07-11 Accepted: 2019-09-24 Published: 2019-11-01

ABSTRACT

The objective of this work is to develop a cost-effective carbonaceous CO_2 adsorbent. N-doped porous carbon (NDC) with nanopore size was synthesized by KOH activation of nano polyaniline (PANI). PANI synthesized in this work has thin nanofibrillar morphology with different lengths and diameters. The activation process was carried out at 800 °C with KOH/precursor ratio of 2. This adsorbent of carbon exhibits high CO_2 adsorption capacity of 1.9 mmol/g at 25 °C under atmospheric pressure. The morphology of PNCs is investigated through different technical methods, such as scanning electron microscopy (SEM), N_2 adsorption isotherm at 77 K and Fourier transform infrared spectroscopy (FTIR). The CO_2 adsorption experiments were done at three different temperatures (298, 308, and 318 K) and pressure up to 10 bar, and correlated with the Langmuir, Freundlich, and Sips models. The Sips isotherm model presented the best fit to the experimental data. Small values of isosteric heat of adsorption were evaluated based on Clausius–Clapeyron equation showed the physical nature of adsorption mechanism. The high amount of CO_2 capture by nanopore size NDC renders it as a promising carrier for practical applications such as gas separation.

Keywords: *Nano Polyaniline; Nitrogen doping; Carbon dioxide adsorption; Chemical activation*

How to cite this article

Khalili S, Jahanshahi M. Nitrogen doped porous carbon derived from polyaniline for CO_2 adsorption. J. Water Environ. Nanotechnol., 2019; 4(4): 285-295. DOI: 10.22090/jwent.2019.04.003

INTRODUCTION

In the past decades, one of the greatest threats to human health is global warming due to cause a significant climate change [1]. To mitigate CO_2 emissions, carbon capture and sequestration (CCS) is considered to be one of the most promising solutions [2]. Fossil fuel-burning power plants are the single largest anthropogenic sources globally among all CO_2 emission sources, accounting for approximately one-third of CO_2 emissions [3]. For the capture of CO_2, amine scrubbing is currently the mature technology, utilizing the chemical reactions between amines and CO_2 [4]. However, the regeneration of the amine solution needs the heating of the system and generates serious energy consumption [5]. In recent years, solid adsorbent materials using chemisorption or physisorption have been intensively investigated such as carbons [6], zeolites [7], metal-organic frameworks (MOFs) [8,9], covalent-organic frameworks (COFs) [10], and porous polymers [11].

Porous carbon as gas sorbent has a long history due to has various advantages such as high surface area, low cost, high conductivity, fast kinetics, diverse availability, facile preparation strategies, outstanding stability, and low manufacturing cost. Polyaniline (PANI) is a conductive polymer with high nitrogen content. It has been intensively investigated in materials science due to its versatile applicability (e.g., sensors [12,13] or conducting wires [14]). These applications are based on their macroscopic properties like electrical conductivity or charge by redox processes [15]. Another potential application of polyaniline concerns its conversion to activated carbons by physical activation or chemical activation with various activating agents

* Corresponding Author Email: *mmohse@yahoo.com*

such as KOH, $ZnCl_2$, Na_2CO_3, K_2CO_3, $NaHCO_3$, NaOH, and H_3PO_4 for CO_2 capture due to its large N content. Among these, KOH is most frequently reported in the literature, because ACs activated by KOH possess well-defined micropore size distributions and ultrahigh specific surface areas [16]. During KOH activation, some of the nitrogen groups reacted with KOH to facilitate KOH penetration into deeper layers of the carbon, leading to a greater development of the micropore structure, while other nitrogen groups were transformed into more thermally stable species and built into the carbon structure. The resulting porous carbons thus featured a high fraction of fine micropores (<1 nm) and some degree of basic nitrogen-containing groups.

Nitrogen doping is a very powerful tool for enriching the functionality of carbon materials. Nitrogen-doped carbons have been widely investigated in different fields [17]. Promising results on their CO_2 adsorption performances have also been reported, nitrogen doping exerts positive influences on both the CO_2 uptake and the adsorption selectivity over other gases [18-20]. The preparation of nitrogen-doped carbon from nitrogen-containing precursor is thus of particular significance.

With this in mind, this study reports the preparation of microporous activated carbon prepared from polyaniline as a carbon source. The adsorption equilibrium data of pure CO_2 on prepared adsorbent was measured volumetrically at different temperatures (298, 308 and 318K) and pressures ranging 1 to 10 bar. The equilibrium and thermodynamic study of the CO_2 adsorption were studied to describe the adsorption processes. To the best of our knowledge, no study has been done on the production of NDC for CO_2 capture from PANI that prepared with DBSNa as a dopant.

EXPERIMENTAL SECTION

Materials

Carbon dioxide and nitrogen were employed with a purity of 99.99% and 99.995%, respectively. Hydrochloric acid 37% (HCl) and potassium hydroxide (KOH) were obtained from Scharlau. Aniline (AR grade), sodium dodecylbenzenesulfonate (DBSNa), ammonium persulphate (APS) and ethanol were purchased from Merck. Also, the water used throughout the work was distilled water.

Synthesis of the N-doped organic porous activated carbon from PANI

The preparation of nano polyaniline was explained in our previous work [21]. For the preparation of PANI, the first aniline was distilled twice under atmospheric pressure to eliminate the oxidation impurities. In this procedure, 1g APS as an oxidant and 0.5 g DBSNa each was dissolved in 50 mL of 1M H_2SO_4 and were stirred for 30 min and then mixed together stirred for 15 min. Then, 1 mL freshly distilled aniline monomer was added to the mixture under vigorous stirring. The reaction vessel was placed in an ice bath during addition oxidant. The reaction mixture was left stirring for about 3 hours at low temperature (0–5 °C). Consequently, the precipitated polymer was filtered and washed with ethanol and distilled water in order to remove oligomers and other non-polymeric impurities until the washing liquid was colorless. The polymer was dried in a vacuum oven at 60 °C for 24 h.

Chemical activation of the PANI was done with impregnating the precursor with KOH. 1 g of the dried precursor was impregnated with 2g KOH and mixed at 80 °C for 3 h. After mixing, the slurry was placed in the vacuum drying at 110 ^{0}C for 20 h. The impregnated precursor was placed in tubular quartz reactor and carbonized up to 800^{0}C at a rate of 5 ^{0}C/min in an electrical furnace for 1h under N_2 flow (100 ml/min STP). After pyrolysis, the activated carbon was cooled down to room temperature in a flow of nitrogen and then removed from the reactor. In all experiments, nitrogen flow rate and heating rate were kept constant. Pyrolysis under inert gas breaks down the cross-link between carbon atoms and avoids the dilution of gas products. The product was washed sequentially with 0.5 M HCl solution to remove the activating agent from the material. The NDC was separated from the solution by filtration and was washed several times with hot and finally cold distilled water until the pH of the filtrate reached around 6.0 and then dried overnight in vacuum oven. The preparation interaction of NDC is schematically illustrated in Fig. 1.

Instrumental characterization

The chemical composition of raw PANI and prepared activated carbon were measured using a CHNS elemental analyzer (Costech ECS 4010, Italy). Functional groups present in the NDC was analyzed using Fourier transform infrared

spectroscopy (Bruker Vertex-70, Germany). The samples were ground and then mixed with KBr, and the spectra were recorded in the range of 400–4000 cm^{-1}. The textural properties of the prepared sorbents were determined from N_2 adsorption isotherm at 77 K using an adsorption apparatus (BELSORP 28, BEL Inc., Japan). Before each measurement, the samples were degassed under a high vacuum at 393 K for 15 h in order to out-gas any remaining moisture or organic species. The specific surface area of the samples was calculated by the application of the Brunauer–Emmett–Teller (BET) method.

Gas adsorption measurement

The CO_2 adsorption performance of the prepared sample was evaluated using volumetric method. The schematic diagram of volumetric apparatus is shown in Fig. 2. The apparatus consisted of two high-pressure stainless steel vessels including the pressure and adsorption cells. Both cells were placed into thermostatic water circulating bath to keep the temperature constant during CO_2 adsorption. The high precision pressure gauge measured the changes in pressure in gas and adsorption cells in each CO_2 adsorption experiment. Prior to CO_2 adsorption experiments, activated carbon was degassed at 100 °C for about 24 h and the system was evacuated by vacuum pump. Helium gas was utilized as non-adsorbing gas to determine the dead volume. The CO_2 adsorption experiments were conducted at pressures ranging from 0 to 10 bar at different temperatures (298–318 K). Using the SRK equation of state in MATLAB

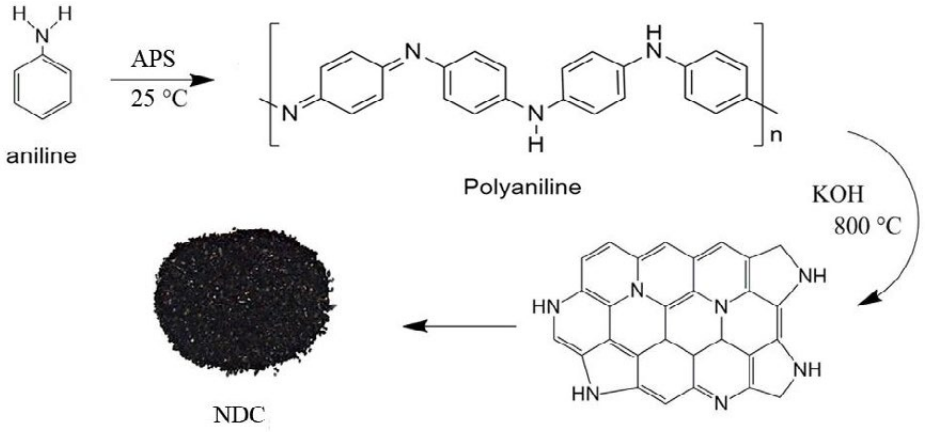

Fig. 1. Schematic illustration of the preparation of porous carbon (NDC).

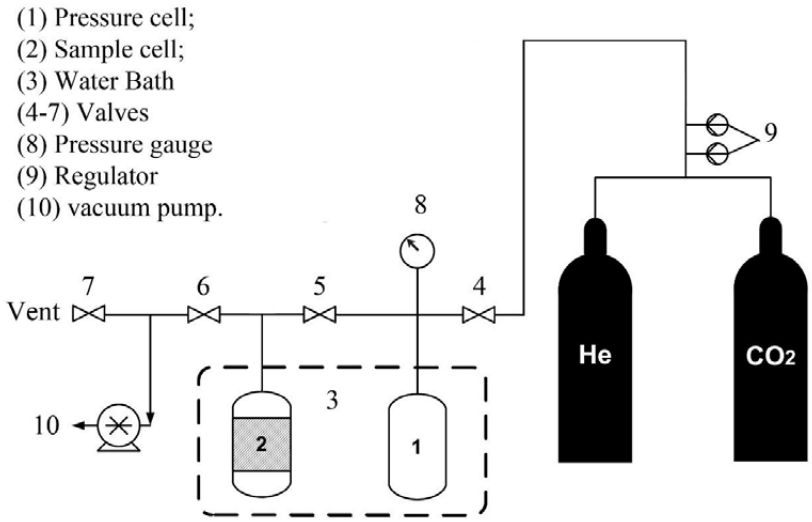

Fig. 2 Schematic diagram of the volumetric adsorption apparatus.

program the amount of CO_2 adsorbed on NDC was calculated.

Adsorption isotherm simulation

The adsorption isotherm shows how the gas molecules distribute between the solid phase and the gas phase when the adsorption process reaches an equilibrium state. An important step to find the appropriate model that can be used for design purposes is an analysis of the experimental isotherm data by fitting them to different isotherm models.

The Langmuir model is based on the assumption that the adsorption occurs at homogeneous sites at the adsorbent surface and adsorption energy is constant and independent of surface coverage. When the surface is covered by a monolayer of adsorbate, the maximum adsorption occurs. The Langmuir model is the most commonly employed equilibrium relation and given by [22]:

$$q = q_m \frac{bP}{1+bP} \quad (1)$$

where q is the amount of CO_2 adsorbed per unit mass of adsorbent (mmol.g^{-1}); q_m is the maximum CO_2 adsorption capacity (mmol.g^{-1}) and b is $b=k_a/k_b$, k_a and k_b are adsorption and desorption constants, respectively.

The empirical Freundlich equation is derived by assuming that there is an exponential variation in site energies of adsorbent and also surface adsorption is not rated limiting step. Freundlich isotherm can be expressed by [23]:

$$q = KP^{\frac{1}{n}} \quad (2)$$

The constant K_F is the adsorption capacity of the adsorbent and n is a measure of the deviation of the model from linearity of the adsorption and indicates sorption intensity. For n equal to unity, the adsorption is linear. If the value is below unity, this confirms that the adsorption process is chemical and the surface is relatively homogeneous. For the value greater than unity, adsorption is a physical process and the sorbent is relatively heterogeneous. In a recent case, adsorbate is favorably adsorbed on the adsorbent. The higher n value shows a stronger adsorption intensity [24, 25].

Sips or Langmuir–Freundlich isotherm [26] can be considered as a combination of the Langmuir and Freundlich isotherm models and describe the heterogeneity of the surface adsorbent. This isotherm model is expressed as follow:

$$q = q_m \frac{bP^{\frac{1}{n}}}{1+bP^{\frac{1}{n}}} \quad (3)$$

where q_m, b, and n were previously described. As mentioned before, for the values of 1/n less than one, the adsorption process is heterogeneous whereas values closer to or even one confirms that there are relatively more homogeneous binding sites in the adsorbent [27].

Thermodynamic of adsorption

Information about the isosteric heat of adsorption as a critical design variable in estimating the performance of an adsorptive gas separation process is necessary for all industrial adsorption processes. The heat of adsorption expresses the changing of enthalpy before and after adsorption between gas molecules and the surface of adsorbent.

The isosteric heat of adsorption of a gas at a specific adsorbate loading can be estimated from the temperature dependence of the isotherm using the Clausius–Clapeyron equation as follows:

$$\Delta H_s = R\left[\frac{d\ln P}{d(\frac{1}{T})}\right]_q \quad (4)$$

where q is the constant adsorbate loading. The isosteric heat of adsorption of CO_2 onto adsorbents can be derived from the slope of the lines in the plots of lnP versus 1/T at a constant adsorbed amount.

RESULTS AND DISCUSSION

SEM imaging was conducted to reveal the evolution of the morphology and surface from NDC. The morphology of nano polyaniline and NDC is shown in Fig. 3. As can be observed from Fig. 3(a), PANI synthesized by rapidly-mixing the solution of oxidant, monomer, and surfactant had thin nanofibrillar morphology with different lengths and diameters. Large pores with different shapes and sizes are randomly distributed in the particle of adsorbent. This observation is associated with the chemical reaction between KOH and the carbon taking place during the activation process, this reaction playing an important role in the development of the porosity in the activated carbon [28].

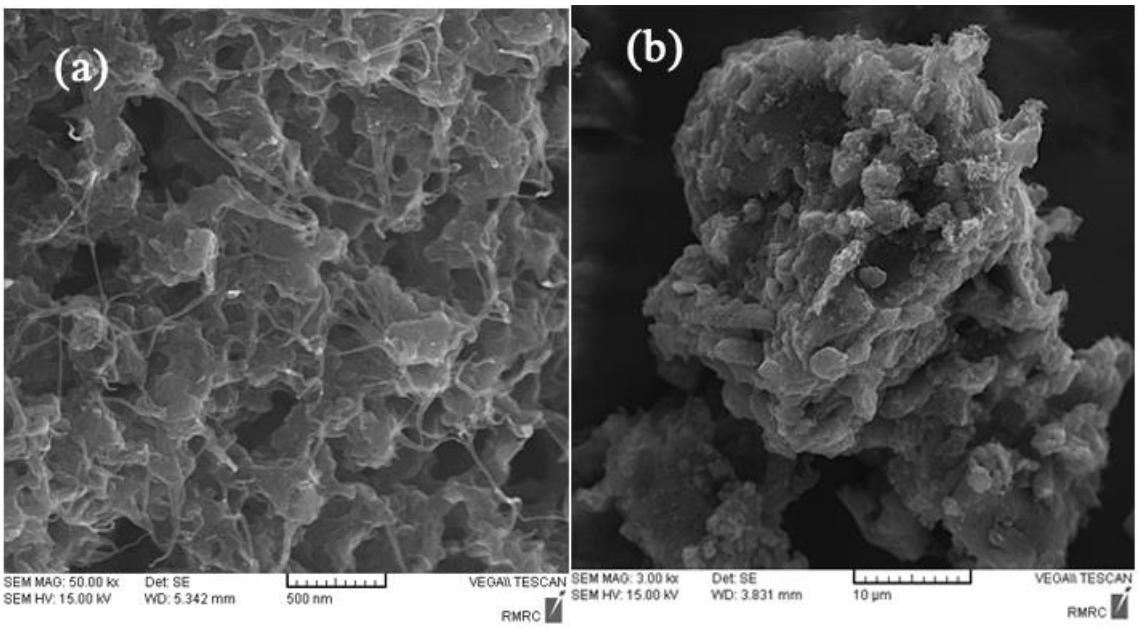

Fig. 3. SEM image of nano polyaniline (a) and prepared NDC (b).

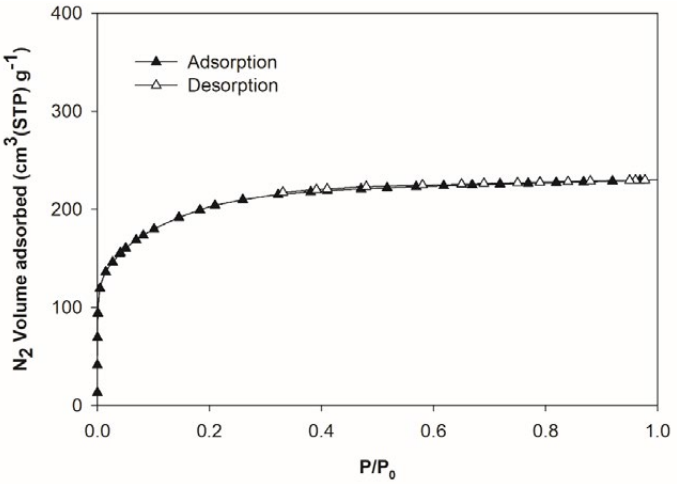

Fig. 4 Adsorption/desorption isotherms of N_2 for NDC.

Fig. 4 shows the N_2 adsorption-desorption isotherms of the NDC prepared from PANI. It can be seen from Fig. 4 that the NDC demonstrates the type I isotherm according to the Brunauer classification, indicating that there are mainly micropores and a relatively small external surface area in the sample. The most uptake of N_2 adsorption was determined in at low relative pressures region, which is considered due to the formation of highly microporous material with narrow pore-size distribution and monolayer adsorption on the NDC. The textural parameters of the prepared sample were shown in Table 1.

The presence of the nitrogen-containing groups can be confirmed by FTIR spectroscopy. Fig.5(a) shows the FTIR spectra of PANI, recorded using KBr pellet. The peaks observed at 1118 and 1295

Table 1. Textural properties of the sample.

BET surface area (m^2/g)	723
Total pore volume (cm^3/g)	0.32
Micropore volume (cm^3/g)	0.30
Mesopore volume(cm^3/g)	0.02
Micropore volume (%)	93
Average pore diameter (nm)	1.8

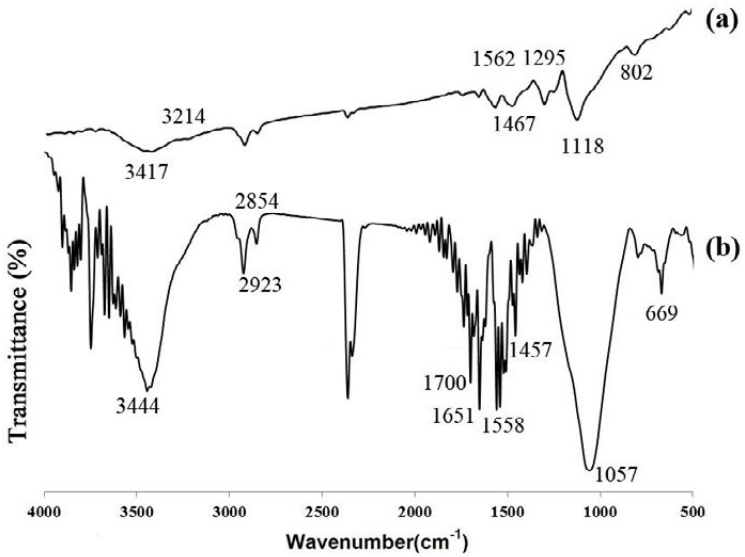

Fig. 5. FTIR spectra of the PANI(a) and NDC (b).

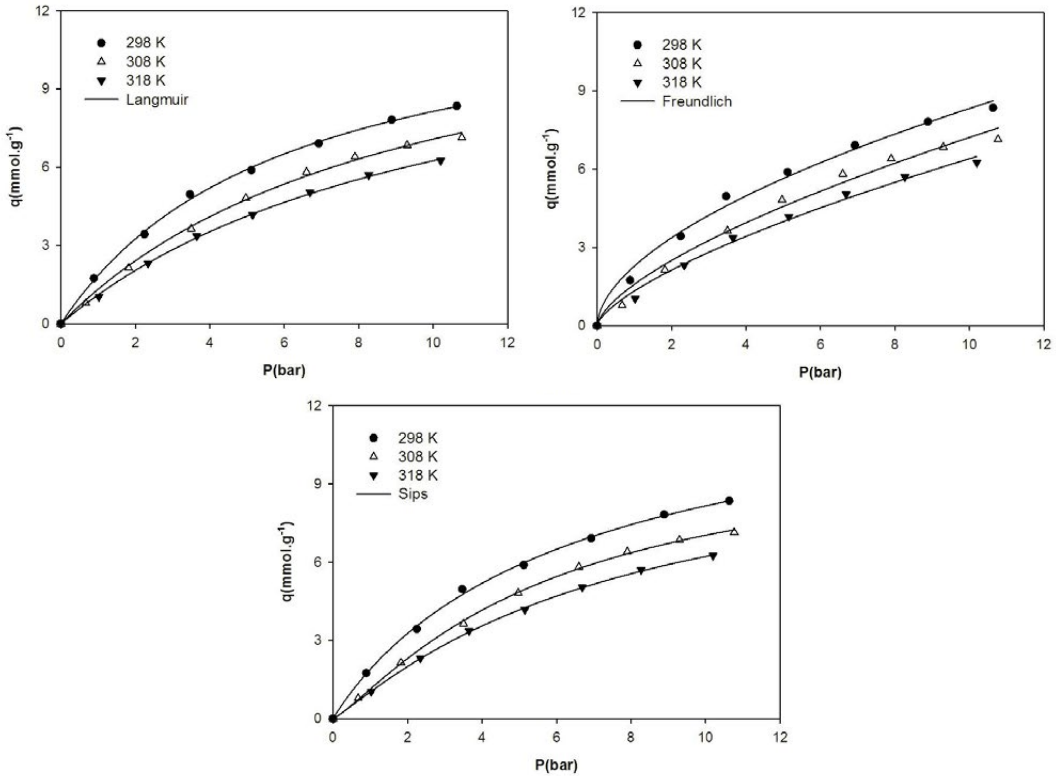

Fig. 6. The nonlinear fit of experimental data with Langmuir, Freundlich, and Sips models.

cm^{-1} are assigned to the C-N stretching vibration. The characteristic peaks at 1467, 1562 and 1650cm^{-1} are assigned to the C=C in the benzene ring and the quinoid ring. The adsorption at 3214 cm^{-1} is due to the N–H stretching vibration. FTIR absorbance spectrum of NDC shows peaks at 1057 cm^{-1} for C–N stretching vibration. The band at 1558 can be identified as originating from the N-H in-plane deformation vibration. The weak bands at 2854 and 2923 cm^{-1} correspond to C-H bond, and the weak band of 1651 cm^{-1} is attributed to the distinctive absorbance of C-H bonds of benzene rings as well

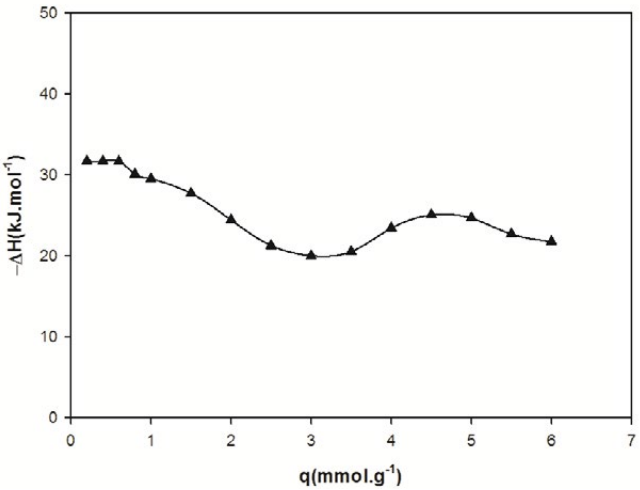

Fig. 7. Isosteric heat of adsorption against surface loading for adsorption of CO_2 onto NDC.

as the C=N bonds from the carbon framework. The peak at 1700 cm^{-1} corresponds to the–C=O stretching vibration. The peak at about 3444 cm^{-1} assigned to the N-H symmetric stretching vibration of –OH stretching vibration [29-33]. The FTIR analysis, therefore, confirms the existence of N-H and C-N species in the carbon sample.

Fig. 6 demonstrates the equilibrium adsorption isotherms of CO_2 on the prepared activated carbon from PANI. Based on the Brunauer classification, all of the CO_2 adsorption isotherms are Type I. This phenomenon is predictable for adsorption of small adsorbates such as CO_2 molecules on a microporous adsorbent. Also, it exhibits a steep increase at low pressure due to existence vacancies or sites available for adsorption. At higher pressure, the amount of gas adsorbed amounts increases slightly because at high pressure most of the sites are occupied. Results demonstrated that the adsorption capacity of CO_2 decreased with increasing the temperature from 298K to 318K, indicating the exothermic nature of the adsorption. In fact, as temperature increased, the physical bonding between the gas molecules (including CO_2) and the active sites of the adsorbent weakened. Therefore, gas molecules adsorbed on the AC surface obtain enough energy to overcome the van der Waals forces and go back to the gas phase. Consequently, the sorption values decreased with temperature increment.

The experimental equilibrium data for CO_2 adsorption on NDC were fitted with Langmuir, Freundlich and Sips isotherm to determine which model gives the best correlation to experimental data. These isotherm models were fitted to experimental data and presented in Fig.6. The parameter values of the three isotherm equations are summarized in Table 2. According to Table 2, the amount of q_m, b, and k for all adsorbents was decreased by increasing the temperature from 298 to 318 K due to existing an inverse relationship between CO_2 adsorption and temperature which approve an exothermic nature of the adsorption process. The Freundlich exponent (n) for AC was more than 1, indicating that CO_2 was favorably adsorbed onto this adsorbent at all temperatures. Based on the regression (R^2) coefficients, the Sips model had the best fit with the experimental data, suggesting the heterogeneous surface of AC [34]. The value of q_{max} obtained from the Langmuir model was slightly higher than that obtained with the Sips model for all adsorbents.

Table 2. The parameter values of the three isotherm equations.

T(K)	Langmuir			Freundlich			Sips			
	q_m(mmol.g^{-1})	b(bar^{-1})	R^2	K(mmol.g^{-1}.$bar^{-1/n}$)	n	R^2	q_m(mmol.g^{-1})	b($bar^{-1/n}$)	n	R^2
298	13.675	0.166	0.998	2.282	1.778	0.992	13.649	0.161	1.211	0.999
308	13.042	0.107	0.998	1.583	1.518	0.988	12.643	0.120	1.114	1.000
318	12.883	0.094	0.999	1.327	1.463	0.993	10.739	0.106	1.037	1.000

CO_2 adsorption mechanism

The improvement in the adsorption capacity of the NDC can be attributed to the chemisorption interaction of CO_2 with amine groups. The reactions occurring between the N-doped AC are basically the same as that between the liquid amine and the CO_2 gas. The overall reaction between the CO_2 molecule and the secondary amine is formation of carbamate. The proposed reaction can be expressed as follows [35]:

$$CO_2 + 2R_1R_2NH \rightarrow R_1R_2NH_2^- + R_1R_2NCO_2^-$$

As can be seen from the reaction, in order to form the carbamate, as the final product, two nitrogen atoms from the amine groups (close enough to each other) are needed. Base on the Dankwerts' zwitterion mechanism the reaction includes a formation of a zwitterion intermediate. Actually, the above reaction is constituted from two reactions:

$$CO_2 + R_1R_2NH \rightarrow R_1R_2NH^+CO_2^-$$
$$R_1R_2NH^+CO_2^- + R_1R_2NH \rightarrow R_1R_2NH_2^- + R_1R_2NCO_2^-$$

Breaking of amine N–H bond and trapping of a proton by another amine group cause to form carbamate. Hence, the process depends on the ability of the amine to split/bind the proton.

Thermodynamic of adsorption

Determination of the heat of adsorption and its variation with coverage can give practical information about surface characteristics and the adsorbed phase. Surface characteristics are measurable by determining the heat of adsorption released from the interaction of adsorbate with the adsorbent at a certain loading.

The isosteric heat of adsorption of CO_2 onto NDC was obtained from the slope of the lines of ln P versus 1/T plot at a constant adsorbed amount. The variation of isosteric heat of adsorption with surface loading was illustrated in Fig. 7. The negative value of the isosteric heat of adsorption suggests the exothermic nature of the process of CO_2 adsorption by adsorbents. The heat of adsorption is interpreted as an indicator of the interaction strength between the gas molecules and the adsorbent. For heat of adsorption of 80 kJ/mole or more, the adsorption process is chemisorption and smaller values are representative of physisorption [36]. According to the ideal Langmuir model, the heat of adsorption is independent of surface coverage. However, this necessity is seldom satisfied in actual systems due to the surface heterogeneity and strong effects of adsorbate - adsorbate interaction.

At lower surface coverage (from 0.2 mmol.g^{-1} up to 0.6 mmol.g^{-1}), the isosteric heat of adsorption of CO_2 exhibits almost constant, thereby indicating a homogeneous adsorption system and there is no lateral interaction between the adsorbed CO_2 molecules. By increasing CO_2 loading, (from 0.8 mmol.g^{-1} up to 3 mmol.g^{-1}), the isosteric heat of adsorption of CO_2 decreased. The weak interaction between CO_2 and adsorbent occurs. Since the strong adsorption sites are occupied first and upon increased loading, the weaker adsorption sites

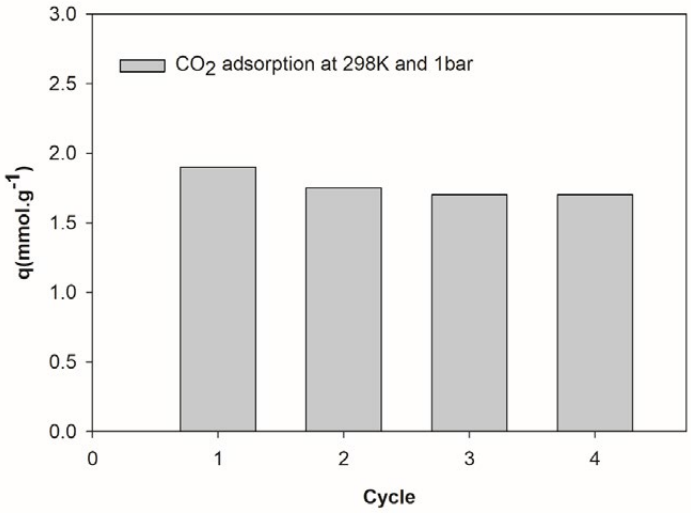

Fig. 8. Cyclic adsorption-desorption tests.

Table 3. Comparison of CO_2 adsorption capacity with other adsorbents.

Adsorbent	Gas composition	T(K)	Adsorption capacity(mmol.g^{-1})	Methods	Ref.
AC	100% CO_2	298	1.91	PSA	20
AC Norit RB1	100% CO_2	294	2.46	gravimetric analysis	38
Anthracite-based AC	100% CO_2	303	1.33	TGA	39
PEI-SBA15	15 v % CO_2, 4.5 v % O_2, 80.5 v % N_2	348	3.14	Fixed bed Flow system	40
TEPA-fumed silica	15%CO_2(4% H2O) in air	348	2.09	TPD-MS	41
AC-A35/4	100% CO_2	293	2.00	Flow desorption	42
PET-MCM-41	100% CO_2	348	2.52	TGA	43
β-Zeolite	100% CO_2	303	1.76	PSA	44
NDC	100% CO_2	298	1.9	PSA	This study

will be occupied. Hence, the heat of adsorption decreases. With increasing CO_2 loading (from 3.5 mmol.g^{-1} up to 4.5 mmol.g^{-1}), the isosteric heat increases slightly due to the adsorbate-adsorbate interactions at higher pressure. By increasing CO_2 loading, (from 5mmol.g^{-1} up to 6 mmol.g^{-1}), the isosteric heat of adsorption of CO_2 decreased. In the present study, the values of isosteric heat of adsorption obtained for NDC were lower than 80 kJ.mol^{-1} indicating that the interaction between NDC and CO_2 molecules is mainly physical interactions involving weak van der Waals and electrostatic interactions.

cyclic operation

From an industrial point of view, an effective adsorbent should be regenerable through several adsorption-desorption cycles. In this work, the study of sorbent regenerability was tested in 4 consecutive cycles at 298 K. After the adsorbent was exposed to the CO_2 adsorption, it was recycled. The recycled adsorbent was then degassed at 100 °C for 24 h before the next cycle of CO_2 adsorption. According to Fig. 8, the adsorption capacities of the sample decrease slightly after the first regeneration and are more or less constant after subsequent regenerations. The decrease in capacity after first regeneration can be attributed to the unreleased CO_2 resulted from the first saturation. Moreover, no significant accumulation of CO_2 is observed during each step of adsorption after first regeneration. This capability of satisfactory regeneration observed from the figure may be considered as a promising sign for stable performance in practical cyclic operations [37].

Comparison of CO_2 adsorption capacity with other adsorbents

The CO_2 uptake performance of the NDC sample synthesized in this work was compared to other adsorbents reported in the literature as summarized in Table 3. Based on Table 3, shows that there are many studies on the adsorption of CO_2 using various types of adsorbent. Nevertheless, the adsorbent capacity for each adsorbent is different due to the different types of raw material and preparation procedures of adsorbents which affect the properties of them. It is clear that the NDC prepared in this study offer a lot of promising benefits for commercial purposes.

CONCLUSION

In conclusion, nitrogen-doped carbon was obtained by chemical activation of the polyaniline as a precursor with KOH. The carbon material activated at 800 °C showed high CO2 uptakes of 1.9 mmol/g^{-1} at 298 K and 1bar. Experimental results were analyzed through Langmuir, Freundlich and Sips models which lead to estimate relative performances of these three isotherm models, describe the experimental results, quantify the gas adsorption on prepared AC and classify them. Prepared adsorbent showed higher adsorption capacity in the whole pressure range and temperature investigated due to the existence of great affinity between CO_2 molecules as a Lewis acid and basic amine sites on the NDC. Values of isosteric heat of adsorption were evaluated based on Clausius–Clapeyron equation. In the present study, the values of isosteric heat of adsorption obtained for NDC were lower than 80 kJ.mol^{-1} indicating that the interaction between NDC and CO_2 molecules is mainly physical interactions involving weak van der Waals and electrostatic interactions. The high amounts of CO_2 capture by NDC render it as a promising carrier for practical applications such as gas separation.

ACKNOWLEDGMENT

The authors gratefully acknowledge Babol Noshirvani University of Technology for financial support of this work through Grant program No. BNUT/370302/98.

CONFLICTS OF INTEREST

There are no conflicts to declare.

REFERENCES

1. Ghosh S, Ramaprabhu S. Green synthesis of transition metal nanocrystals encapsulated into nitrogen-doped carbon nanotubes for efficient carbon dioxide capture. Carbon. 2019;141:692-703.
2. Ma X, Wang X, Song C. "Molecular Basket" Sorbents for Separation of CO2and H2S from Various Gas Streams. Journal of the American Chemical Society. 2009;131(16):5777-83.
3. Pires J, Juźków J, Pinto ML. Amino acid modified montmorillonite clays as sustainable materials for carbon dioxide adsorption and separation. Colloids and Surfaces A: Physicochemical and Engineering Aspects. 2018;544:105-10.
4. Dutcher B, Fan M, Russell AG. Amine-Based CO2 Capture Technology Development from the Beginning of 2013—A Review. ACS Applied Materials & Interfaces. 2015;7(4):2137-48.
5. Sreedhar I, Aniruddha R, Malik S. Carbon capture using amine modified porous carbons derived from starch (Starbons®). SN Applied Sciences. 2019;1(5).
6. Radosz M, Hu X, Krutkramelis K, Shen Y. Flue-Gas Carbon Capture on Carbonaceous Sorbents: Toward a Low-Cost Multifunctional Carbon Filter for "Green" Energy Producers†. Industrial & Engineering Chemistry Research. 2008;47(10):3783-94.
7. Sarker AI, Aroonwilas A, Veawab A. Equilibrium and Kinetic Behaviour of CO2 Adsorption onto Zeolites, Carbon Molecular Sieve and Activated Carbons. Energy Procedia. 2017;114:2450-9.
8. Li H, Wang K, Sun Y, Lollar CT, Li J, Zhou H-C. Recent advances in gas storage and separation using metal–organic frameworks. Materials Today. 2018;21(2):108-21.
9. Sumida K, Rogow DL, Mason JA, McDonald TM, Bloch ED, Herm ZR, et al. Carbon Dioxide Capture in Metal–Organic Frameworks. Chemical Reviews. 2011;112(2):724-81.
10. Dash B. Carbon dioxide capture using covalent organic frameworks (COFs) type material—a theoretical investigation. Journal of Molecular Modeling. 2018;24(5).
11. Shao L, Wang S, Liu M, Huang J, Liu Y-N. Triazine-based hyper-cross-linked polymers derived porous carbons for CO2 capture. Chemical Engineering Journal. 2018;339:509-18.
12. Liu Y, Zhao X, Tuo X. Preparation of polypyrrole coated cotton conductive fabrics. The Journal of The Textile Institute. 2016;108(5):829-34.
13. Vidal JC, Garcıa E, Castillo JR. In situ preparation of a cholesterol biosensor: entrapment of cholesterol oxidase in an overoxidized polypyrrole film electrodeposited in a flow system. Analytica Chimica Acta. 1999;385(1-3):213-22.
14. Jérôme C, Labaye D, Bodart I, Jérôme R. Electrosynthesis of polyacrylic/polypyrrole composites: Formation of polypyrrole wires. Synthetic Metals. 1999;101(1-3):3-4.
15. Dodouche I, Epron F. Promoting effect of electroactive polymer supports on the catalytic performances of palladium-based catalysts for nitrite reduction in water. Applied Catalysis B: Environmental. 2007;76(3-4):291-9.
16. Lv Y, Zhang F, Dou Y, Zhai Y, Wang J, Liu H, et al. A comprehensive study on KOH activation of ordered mesoporous carbons and their supercapacitor application. J Mater Chem. 2012;22(1):93-9.
17. Wood KN, O'Hayre R, Pylypenko S. Recent progress on nitrogen/carbon structures designed for use in energy and sustainability applications. Energy Environ Sci. 2014;7(4):1212-49.
18. Ashourirad B, Arab P, Islamoglu T, Cychosz KA, Thommes M, El-Kaderi HM. A cost-effective synthesis of heteroatom-doped porous carbons as efficient CO2 sorbents. Journal of Materials Chemistry A. 2016;4(38):14693-702.
19. Ashourirad B, Sekizkardes AK, Altarawneh S, El-Kaderi HM. Exceptional Gas Adsorption Properties by Nitrogen-Doped Porous Carbons Derived from Benzimidazole-Linked Polymers. Chemistry of Materials. 2015;27(4):1349-58.
20. Khalili S, Khoshandam B, Jahanshahi M. Optimization of production conditions for synthesis of chemically activated carbon produced from pine cone using response surface methodology for CO2 adsorption. RSC Advances. 2015;5(114):94115-29.
21. Khalili S, Khoshandam B, Jahanshahi M. Synthesis of activated carbon/polyaniline nanocomposites for enhanced CO2 adsorption. RSC Advances. 2016;6(42):35692-704.
22. Shao D, Ren X, Wen J, Hu S, Xiong J, Jiang T, et al. Immobilization of uranium by biomaterial stabilized FeS nanoparticles: Effects of stabilizer and enrichment mechanism. Journal of Hazardous Materials. 2016;302:1-9.
23. Mahmoodi NM, Hayati B, Arami M. Kinetic, equilibrium and thermodynamic studies of ternary system dye removal using a biopolymer. Industrial Crops and Products. 2012;35(1):295-301.
24. Madaeni SS, Salehi E. Adsorption of cations on nanofiltration membrane: Separation mechanism, isotherm confirmation and thermodynamic analysis. Chemical Engineering Journal. 2009;150(1):114-21.
25. Ahmad MA, Alrozi R. Optimization of preparation conditions for mangosteen peel-based activated carbons for the removal of Remazol Brilliant Blue R using response surface methodology. Chemical Engineering Journal. 2010;165(3):883-90.
26. López-Muñoz M-J, Arencibia A, Cerro L, Pascual R, Melgar Á. Adsorption of Hg(II) from aqueous solutions using TiO2 and titanate nanotube adsorbents. Applied Surface Science. 2016;367:91-100.
27. Tan IAW, Ahmad AL, Hameed BH. Adsorption of basic dye on high-surface-area activated carbon prepared from coconut husk: Equilibrium, kinetic and thermodynamic studies. Journal of Hazardous Materials. 2008;154(1-3):337-46.
28. Li L, Liu E, Shen H, Yang Y, Huang Z, Xiang X, et al. Charge storage performance of doped carbons prepared from polyaniline for supercapacitors. Journal of Solid State Electrochemistry. 2010;15(1):175-82.
29. Chang B, Shi W, Yin H, Zhang S, Yang B. Poplar catkin-derived self-templated synthesis of N-doped hierarchical porous carbon microtubes for effective CO2 capture. Chemical Engineering Journal. 2019;358:1507-18.
30. Alabadi A, Abbood HA, Li Q, Jing N, Tan B. Imine-Linked Polymer Based Nitrogen-Doped Porous Activated Carbon for Efficient and Selective CO2 Capture. Scientific Reports. 2016;6(1).
31. Liu L, Deng Q-F, Ma T-Y, Lin X-Z, Hou X-X, Liu Y-P, et al. Ordered mesoporous carbons: citric acid-catalyzed synthesis, nitrogen doping and CO2 capture. Journal of

Materials Chemistry. 2011;21(40):16001.
32. Shen W, Zhang S, He Y, Li J, Fan W. Hierarchical porous polyacrylonitrile-based activated carbon fibers for CO2 capture. Journal of Materials Chemistry. 2011;21(36):14036.
33. Yu J, Guo M, Muhammad F, Wang A, Zhang F, Li Q, et al. One-pot synthesis of highly ordered nitrogen-containing mesoporous carbon with resorcinol–urea–formaldehyde resin for CO2 capture. Carbon. 2014;69:502-14.
34. Ahmed MJ, Dhedan SK. Equilibrium isotherms and kinetics modeling of methylene blue adsorption on agricultural wastes-based activated carbons. Fluid Phase Equilibria. 2012;317:9-14.
35. Zelenak V, Halamova D, Gaberova L, Bloch E, Llewellyn P. Amine-modified SBA-12 mesoporous silica for carbon dioxide capture: Effect of amine basicity on sorption properties. Microporous and Mesoporous Materials. 2008;116(1-3):358-64.
36. Spessato L, Bedin KC, Cazetta AL, Souza IPAF, Duarte VA, Crespo LHS, et al. KOH-super activated carbon from biomass waste: Insights into the paracetamol adsorption mechanism and thermal regeneration cycles. Journal of Hazardous Materials. 2019;371:499-505.
37. Irani M, Jacobson AT, Gasem KAM, Fan M. Facilely synthesized porous polymer as support of poly(ethyleneimine) for effective CO2 capture. Energy. 2018;157:1-9.
38. Van Der Vaart, R., C. Huiskes, H. Bosch and T. Reith, 2000. Single and mixed gas adsorption equilibria of carbon dioxide/methane on activated carbon. Adsorption, 6 (4): 311-323.
39. Maroto-Valer MM, Tang Z, Zhang Y. CO2 capture by activated and impregnated anthracites. Fuel Processing Technology. 2005;86(14-15):1487-502.
40. Wang X, Ma X, Song C, Locke DR, Siefert S, Winans RE, et al. Molecular basket sorbents polyethylenimine–SBA-15 for CO2 capture from flue gas: Characterization and sorption properties. Microporous and Mesoporous Materials. 2013;169:103-11.
41. Xu X, Song C, Andresen JM, Miller BG, Scaroni AW. Novel Polyethylenimine-Modified Mesoporous Molecular Sieve of MCM-41 Type as High-Capacity Adsorbent for CO2Capture. Energy & Fuels. 2002;16(6):1463-9.
42. Heuchel M, Davies GM, Buss E, Seaton NA. Adsorption of Carbon Dioxide and Methane and Their Mixtures on an Activated Carbon: Simulation and Experiment. Langmuir. 1999;15(25):8695-705.
43. Son W-J, Choi J-S, Ahn W-S. Adsorptive removal of carbon dioxide using polyethyleneimine-loaded mesoporous silica materials. Microporous and Mesoporous Materials. 2008;113(1-3):31-40.
44. Xu X, Zhao X, Sun L, Liu X. Adsorption separation of carbon dioxide, methane and nitrogen on monoethanol amine modified β-zeolite. Journal of Natural Gas Chemistry. 2009;18(2):167-72.